BBA - Molecular Basis of Disease 1870 (2024) 167116

Contents lists available at ScienceDirect

BBA - Molecular Basis of Disease

journal homepage: www.elsevier.com/locate/bbadis

AurkA/TPX2 co-overexpression in nontransformed cells promotes genome instability through induction of chromosome mis-segregation and attenuation of the p53 signalling pathway

Francesco Davide Naso [a,1,2], Federica Polverino [a,1], Danilo Cilluffo [a], Linda Latini [a], Venturina Stagni [a,b], Italia Anna Asteriti [a], Alessandro Rosa [c,d], Silvia Soddu [e], Giulia Guarguaglini [a,*]

[a] Institute of Molecular Biology and Pathology, National Research Council of Italy, c/o Sapienza University of Rome, Via degli Apuli 4, 00185 Rome, Italy
[b] Istituto di Ricovero e Cura a Carattere Scientifico (IRCCS), Fondazione Santa Lucia, Signal Transduction Unit, Via del Fosso di Fiorano 64/65, 00143 Rome, Italy
[c] Center for Life Nano- & Neuro-Science, Fondazione Istituto Italiano di Tecnologia (IIT), Viale Regina Elena, 291, 00161 Rome, Italy
[d] Department of Biology and Biotechnologies "Charles Darwin", Sapienza University of Rome, Piazzale Aldo Moro 5, 00185 Rome, Italy
[e] Unit of Cellular Networks and Molecular Therapeutic Targets, IRCCS Regina Elena National Cancer Institute, Rome, Italy

ARTICLE INFO

Keywords:
Aurora-A/TPX2 complex
Chromosome mis-segregation
Micronucleus
Mitosis
p53

ABSTRACT

The Aurora-A kinase (AurkA) and its major regulator TPX2 (Targeting Protein for Xklp2) are key mitotic players frequently co-overexpressed in human cancers, and the link between deregulation of the AurkA/TPX2 complex and tumourigenesis is actively investigated. Chromosomal instability, one of the hallmarks of cancer related to the development of intra-tumour heterogeneity, metastasis and chemo-resistance, has been frequently associated with TPX2-overexpressing tumours. In this study we aimed to investigate the actual contribution to chromosomal instability of deregulating the AurkA/TPX2 complex, by overexpressing it in nontransformed hTERT RPE-1 cells. Our results show that overexpression of both AurkA and TPX2 results in increased AurkA activation and severe mitotic defects, compared to AurkA overexpression alone. We also show that AurkA/TPX2 co-overexpression yields increased aneuploidy in daughter cells and the generation of micronucleated cells. Interestingly, the p53/p21 axis response is impaired in AurkA/TPX2 overexpressing cells subjected to different stimuli; consistently, cells acquire increased ability to proliferate after independent induction of mitotic errors, *i.e.* following nocodazole treatment. Based on our observation that increased levels of the AurkA/TPX2 complex affect chromosome segregation fidelity and interfere with the activation of a pivotal surveillance mechanism in response to altered cell division, we propose that co-overexpression of AurkA and TPX2 *per se* represents a condition promoting the generation of a genetically unstable context in nontransformed human cells.

1. Introduction

Chromosomal instability (CIN) is a cancer-driver condition strictly linked with tumour aggressiveness, metastatisation, relapses and chemo-resistance [1,2]. CIN can originate from multiple routes [3] and is strongly associated with the occurrence of mitotic errors [4], that also represent a typical feature of cancer cells [5]. Indeed, a strong correlation between alteration of mitotic genes and CIN has been highlighted in cancer [6,7]. Two of these genes, *AURKA* and *TPX2* encode for the subunits of a hetero-complex involved in spindle assembly and mitotic execution [8]. Aurora Kinase A (AurkA) is a serine-threonine kinase with well characterised functions in centrosomes maturation, mitotic entry and progression [9]. TPX2 (Targeting Protein for Xklp2), a microtubule (MT) binding protein, plays a pivotal role in spindle assembly and mitosis execution and is the best characterised regulator of AurkA [8,10]. With its N-terminal region, TPX2 binds AurkA, thereby recruiting the kinase on spindle microtubules [11,12], stabilising its protein levels [13] and its active conformation [14,15]. AurkA and TPX2 are

* Corresponding author.
E-mail address: giulia.guarguaglini@uniroma1.it (G. Guarguaglini).
[1] These authors contributed equally to this work.
[2] Present address: IRCCS Fondazione Santa Lucia, Via del Fosso di Fiorano 64/65, 00143, Rome, Italy.

https://doi.org/10.1016/j.bbadis.2024.167116
Received 8 September 2023; Received in revised form 19 February 2024; Accepted 1 March 2024
Available online 4 March 2024

frequently co-overexpressed in several tumour types, in some cases due to gain of chromosome 20q, where the coding genes are located [16–21]. This has suggested a possible involvement of the AurkA/TPX2 complex as an oncogenic unit in cancer [22], with a potential interest as therapeutic target [23–25]. Of note, TPX2 increased expression displays the highest association score with CIN tumours, ranking first in the identified CIN70 signature [6]. Despite this link, overexpressing TPX2 in nontransformed cells mainly affects mitotic progression and nuclear reconstitution at mitotic exit with no apparent effect on chromosome segregation or micronuclei induction [26]. On the other hand, co-overexpression of other tumour-promoting factors, as proposed for MYC [27], may modify the outcome of high TPX2 expression, thereby promoting CIN. Interestingly, a CIN4 chromosomal instability signature of overexpressed genes, derived from the previously mentioned CIN70, includes both TPX2 and AurkA and defines tumour aneuploidy, with prognostic value in breast cancer patients [28]. Significance of the whole AurkA/TPX2 signalling axis for the survival of chromosomal unstable cancer cells was also recently proposed, with viability of BRCA2-deficient cancer cells being reduced by depletion of either component [29]. On these bases, in this work we explored the possibility that AurkA/TPX2 co-overexpression is particularly relevant for the generation and propagation of CIN in nontransformed cells, compared with overexpression of the single components. To this aim, we chose the near-diploid nontransformed, genetically stable, hTERT RPE-1 cell line previously used for the investigation of TPX2 overexpression effects [26], and induced overexpression of the whole complex, or AurkA alone. We show that excess AurkA requires TPX2 co-overexpression to achieve increased and aberrantly distributed kinase activity in mitotic cells, which interferes with the chromosome segregation process, yielding generation of micronucleated cells. Interestingly, AurkA overexpression also interferes with p53 stabilisation and impairs its response to cellular stresses including mitotic delay or nocodazole-induced chromosomal instability. Together these data suggest the possibility that genomically unbalanced cells generated by high levels of the AurkA/TPX2 complex also harbour tolerance to stress that enables their proliferation, thus contributing to the establishment of a protumourigenic genetically unstable context.

2. Materials and methods

2.1. Cell cultures, synchronisation protocols and treatments

The human hTERT RPE-1 - epithelial cell line immortalised with hTERT- (kind gift of Prof. Jonathon Pines) and the derived stable cell lines for inducible overexpression of AurkA and/or TPX2 [21,26,30], were grown at 37 °C and 5 % CO_2 in complete DMEM/F12 (Dulbecco's Modified Eagle Medium F-12) supplemented with 10 % tetracycline-free foetal bovine serum (FBS). Stable hTERT-immortalised dermal fibroblasts (HF) [31] overexpressing AurkA alone or in combination with FLAG-TPX2 in an inducible manner were generated using the previously described plasmids and procedure [26,30]. Culture conditions were as above, in complete DMEM medium.

Expression of exogenous proteins was induced by administration of 1 μg/ml doxycycline hyclate (tetracycline analogue; Santa Cruz Biotechnology) for 24 h, unless otherwise indicated. Stable transgenic hTERT RPE-1 cell lines for constitutive expression of AurkA and TPX2 were generated by infection with the lentiviral vectors pLV[Exp]-Puro-CMV > hAURKA (VB900000-1420ztx, VectorBuilder) and pLV[Exp]-Bsd-EF1A > hTPX2 (VB900120-6505ssf, VectorBuilder). Cells infected with empty pLV vector were used as control. Culture conditions were as above with 10 % FBS.

When indicated, cells were treated as follows (a) 100 μM monastrol (Tocris) for 12 h to arrest cells in prometaphase; (b) 2 mM thymidine (Sigma-Aldrich) for 24 h followed by 10 h release in thymidine-free medium and mechanical shake-off, to collect and re-plate mitotic cells; (c) for Fig. 4F, 8 h after thymidine wash out monastrol was added for 12 h; cells were subsequently collected by mechanical shake-off, replated in drug-free medium and harvested after 10 h; (d) 1 nM MLN8237 (Selleck Chemical) for 24 h to partially inhibit the kinase activity of AurkA; (e) 100 ng/ml nocodazole (Sigma-Aldrich) for 12 h, to arrest cells in prometaphase, followed by wash-out in drug free-medium and harvesting after 24 h. To perform the BrdU incorporation assay, mitotic nocodazole-treated cells were collected through mechanical shake-off, re-plated in a BrdU-containing medium (Sigma-Aldrich, 5 μM), and fixed at the indicated time points; (f) 0.5 μM Camptothecin (CPT, Sigma Aldrich) for 20 h to induce DNA damage; (g) 20 μM Nutlin-3 (Cayman Chemical) was used for 20 h to induce p53 stabilisation.

2.2. Real-time PCR

Total RNA was extracted and reverse-transcribed as described in [32]. Primers were designed as follows:

p21-FW: 5′-TGGAGACTCTCAGGGTCGAAA-3′;
p21-REV: 5′-GGCGTTTGGAGTGGTAGAAATC-3′.
p53-FW: 5′-GTCTGGGCTTCTTGCATTCT-3′;
p53-REV: 5′-AATCAACCCACAGCTGCA-3′.
TBP-FW: 5′-TGCCCGAAACGCCGAATATAATC-3′;
TBP-REV: 5′-TGGTTCGTGGCTCTCTTATCCTC-3′.

Relative quantification was performed by the comparative cycle threshold method [33]. The mRNA expression values were normalised to those of the TBP (TATA-box–binding protein) gene used as an endogenous control. One control mRNA derived from control cells treated with DMSO, was randomly chosen as control calibrator.

2.3. Immunofluorescence

Cells grown on coverslips were fixed by (i) -20 °C methanol, 6 min or (ii) 3.7 % formaldehyde/30 mM sucrose in PBS, 10 min at room temperature, followed by permeabilisation in PBS containing 0.1 % TritonX-100, 5 min at room temperature. Blocking and incubations with primary and fluorescently-labelled secondary antibodies were performed at room temperature in PBS containing 0.05 % Tween and 3 % BSA. Cells were counterstained with 4,6-diamidino-2-phenylindole (DAPI, 0.1 μg/ml; Sigma-Aldrich) and mounted using Vectashield (Vector Laboratories). Primary antibody incubations were carried out for 1 h, except for γH2AX, p53 and p21 detection (overnight incubation at +4 °C) and centrin detection (2 h at RT). Primary antibodies and used concentrations/dilutions are listed in Table 1. Samples were analysed using (i) a Nikon Eclipse 90i microscope equipped with 20× (N.A. 0.5), 40× (N.A. 0.75) and 100× (oil immersion; N.A. 1.3) objectives and a Qicam Fast 1394 CCD camera (QImaging) or (ii) with an inverted microscope (Eclipse Ti, Nikon) using a 60× (oil immersion, N.A. 1.4) objective and a DS-Qi1Mc camera (Nikon) or (iii) with a confocal spinning disk microscope (Crest X-Light V3) equipped with the Kinetix sCMOS camera (Teledyne Photometrics), a 60× (oil immersion, N.A. 1.4) objective and CELESTA lasers (Lumencor). Images were acquired using Nis-Elements AR (Nikon); elaboration and processing were performed using Nis-Elements HC (Nikon), using the 2D deconvolution module, and Adobe Photoshop CS 8.0.

2.4. In situ proximity ligation assay (isPLA)

In situ proximity ligation assay (*is*PLA) was performed on cells grown on coverslips and fixed with formaldehyde (see previous section) using the Duolink PLA kit (DUO92007, Sigma-Aldrich) according to manufacturer's instructions. The amplification time was 45 min and the primary antibodies pair to detect the interaction was mouse anti-Aurora-A/rabbit anti-TPX2. In the same reactions, IF staining of the spindle was performed using a chicken anti-α-tubulin antibody. Used primary antibodies concentrations/dilutions are listed in Table 1. DNA was stained with DAPI as above. For quantification of *is*PLA fluorescence signals, images of mitotic cells were acquired using a 60× objective (oil

Table 1
Primary antibodies list.

Antibody	Company	Application	Dilution	Identifier
Mouse anti-Aurora-A	BD Bioscience	IF/*is*PLA WB	0.5 μg/ml 0.2 μg/ml	Cat#610939; RRID: AB_398251
Rabbit anti-phospho-Aurora-A (Thr288)	Cell Signalling Technology	IF WB	1:100 1:500	Cat#3079 clone C39D8; RRID: AB_2061481
Anti-BrdU	Dako	IF	1:50	Cat# M0744; RRID: AB_10013660
Mouse anti-centrin	Millipore	IF	1 μg/ml	Cat#04-1624; RRID: AB_10563501
Human anti-centromere	Antibodies Incorporated	IF	1:20	Cat#15234; RRID: AB_2687472
Mouse anti-cyclin B1	BD Biosciences	WB	1:200	Cat# GNS1, 554177; RRID: AB_395288
Mouse anti-γH2AX	Millipore	IF	1:300	Cat#05636; RRID: AB_309864
Mouse anti-GAPDH	Santa Cruz Biotechnology	WB	1:1000	Cat#Sc32233; RRID: AB_627679
Rabbit anti-lamin B1	Abcam	IF	1 μg/ml	Cat#ab16048; RRID: AB_443298
Rabbit anti-p21	Cell Signalling Technology	IF and WB	1:1000	Cat#2947; RRID: AB_823586
Mouse anti-p53	Cell Signalling Technology	IF WB	1:300 1:1000	Cat#48818; RRID: AB_2713958
Rabbit anti-pericentrin	Abcam	IF	1 μg/ml	Cat#Ab4448; RRID: AB_304461
Rabbit anti-TPX2	Novus Biologicals	IF/*is*PLA WB	1:1500 1:500	Cat#NB500-179; RRID: AB_527246
Mouse anti-α-tubulin	Sigma-Aldrich	IF	2 μg/ml	Cat#T5168; RRID: AB_477579
Mouse anti-α-tubulin-FITC	Sigma-Aldrich	IF	20 μg/ml	Cat#F2168; RRID: AB_476967
Chicken anti-α-tubulin	Abcam	IF	1:100	Cat#Ab89984; RRID: AB_10672056

immersion; N.A. 1.4), along the z-axis every 0.4 μm for a range of 8 μm. The "general analysis" module of NIS-Elements H.C. 5.11 was used for automatic recognition and counting of interaction dots inside the whole cell in the Maximum Intensity Projection images.

2.5. Metaphase spread

Cells were treated with 0.2 μg/ml colchicine (Sigma-Aldrich) for 4 h, trypsinized and harvested by centrifugation at 400*g* for 10 min. Cells were swollen by adding 75 mM KCl dropwise and incubated at 37 °C for 10 min, then centrifuged at 250*g* for 10 min. Cell pellet was resuspended adding dropwise 5 ml of cold Carnoy's fixative [methanol/acetic acid (3:1 v/v)] and incubated for 10 min on ice. After repeating the last step twice, cells were dropped onto iced slides. After the slides have dried, chromosomes were stained with 3 % Giemsa solution (VHR Chemicals).

2.6. Fluorescence in situ hybridization (FISH)

Cells grown on slides were swollen by adding 75 mM KCl dropwise and incubated at 37 °C for 10 min, then fixed by adding cold Carnoy's fixative [methanol/acetic acid (3:1 v/v)] dropwise and incubating slides for 10 min on ice. After repeating the last step twice, the slides were air dried and stored at −20 °C for a week. The slide-mounted cells were treated with RNaseA [100 μg/ml in 2× saline-sodium citrate (SSC) buffer] at 37 °C for 30 min, dehydrated in a 70 %/80 %/100 % ethanol series, treated with proteinase K (0.6 μg/ml in 2× SSC) for 5 min at 37 °C and dehydrated again in a 70 %/80 %/100 % ethanol series. The DNA was denatured by slides immersion in 70 % formamide for 5 min at 70 °C. Denatured slides were dehydrated in ice-cold 70 %/90 %/100 % ethanol series and then air dried. The probe mixture (XCE 7/8 DNA probe, Metasystems) was applied to dried slides, before a coverslip was added and sealed with rubber cement. Slides were heated on a hotplate at 75 °C (±1 °C) for 2 min and incubated at 37 °C. Following overnight incubation at 37 °C, the slides were incubated in 0.4× SSC at 72 °C for 2 min and washed in 2× SSC/0.5 % Tween-20 at room temperature for 30 s, then rinsed briefly in distilled water. After the slides have dried, cells were counterstained with 4,6-diamidino-2-phenylindole (DAPI, 0.1 μg/ml; Sigma-Aldrich). Images were acquired using a confocal spinning disk microscope (Crest X-Light V3) equipped with the Kinetix sCMOS camera (Teledyne Photometrics), a 60× (oil immersion, N.A. 1.4) objective and CELESTA lasers (Lumencor).

2.7. Time lapse video-recording microscopy

Cells seeded in 4-well micro-slides (Ibitreat, 80426, Ibidi) were observed with an inverted microscope (Eclipse Ti, Nikon) using a 40× (Plan Fluor, N.A. 0.60, DIC) objective (Nikon). During the whole registration cells were kept in a microscope incubator (Basic WJ, Okolab) at 37 °C in 5 % CO_2. DIC images were acquired every 5 min over 48 h using a Clara camera (ANDOR technology), and the NIS-Elements AR 3.22 software (Nikon). Movie processing and analysis were performed with Nis-Elements HC 5.02 (Nikon).

2.8. Western blotting

Cells were lysed in RIPA buffer (50 mM Tris–HCl pH 8.0, 150 mM NaCl, 1 % NP40, 1 mM EGTA system, 0.25 % sodium deoxycholate) supplemented with protease and phosphatase inhibitors (Roche Diagnostic). Proteins were resolved by 10 or 12 % SDS PAGE and transferred on a nitrocellulose membrane (Protran BA83, GE Healthcare) using a semi-dry system (Bio-Rad). Blocking and antibody incubations were performed at room temperature in Tris-buffered saline (TBS) containing 0.1 % Tween and 5 % low fat milk, except for p-Thr288 AurkA (Tris-buffered saline (TBS) containing 0.1 % Tween and 5 % BSA). Primary antibody incubations were carried out for 1 h, except for p53 and p21 detection (overnight incubation at +4 °C). Primary antibodies and used concentrations/dilutions are listed in Table 1. HRP-conjugated secondary antibodies (Santa Cruz Biotechnology, Bio-Rad) were revealed using the Clarity Western ECL Substrate (Bio-Rad, 1705061). Adobe Photoshop CS 8.0 software was used for the analysis. For each band within the same filter, the same selection area was used. The signal intensity was measured and background was subtracted. Signals were normalised on the GAPDH (loading control) signal.

2.9. FACS analysis

Preparation and analysis of propidium iodide-stained samples was performed as described in [21].

2.10. Statistical analyses

Data were statistically analysed using the InStat3 Graphpad 7 by: (i) unpaired *t*-tests and ordinary one-way ANOVA multiple comparison tests for measurements of continuous variables; when samples were not normally distributed, the Mann–Whitney and Kruskal–Wallis tests, respectively, were used instead; (ii) χ^2 (Fisher's exact) tests, in the contingency tables analyses for measurements of categorical variables. The number of replicates and sample size are indicated in the corresponding figure legends. The criterion for statistical significance (*) was set at $p < 0.01$.

Statistical analysis of Western blot data was performed using the

InStat3 Graphpad 7, with unpaired *t*-test and ordinary one-way ANOVA multiple comparison test, with a criterion for statistical significance (*) set at $p < 0.05$.

3. Results

3.1. Overexpression of AurkA or AurkA/TPX2 differentially affects spindle assembly and chromosome segregation

AurkA and TPX2 increased levels are observed in human cancers and tumour cells, with frequent occurrence of co-overexpression [16–18,22,24]. In order to address the consequences of AurkA and TPX2 co-overexpression on the mitotic process and chromosome segregation fidelity in a nontransformed background, we generated near-diploid hTERT RPE-1 cell lines genetically engineered to obtain increased levels of AurkA alone or in combination with TPX2 (AurkA/TPX2) after doxycycline (dox) administration [21,30]. As a control we used the same cells cultured without dox (referred to as CTR) while the TPX2 alone expressing RPE-1 cells have been previously described [26].

Increased levels of AurkA and TPX2 in the overexpressing cells after 24 h of induction were verified by Western blot (WB) in extracts from interphases, or mitotic –monastrol arrested– cells, collected by mechanical shake-off (Fig. 1A and Fig. S1). This corresponded to a strong increase in AurkA/TPX2 complex formation on the mitotic spindle, as assessed by *in situ* Proximity Ligation Assay (*is*PLA), with respect not only to CTR mitoses but also to prometa-metaphases (PM/Ms) overexpressing AurkA alone (Fig. 1B). Interestingly, the mitotic localisation of AurkA, when overexpressed with TPX2, was not restricted to the spindle poles, but extended along MTs, following TPX2 localisation at the mitotic spindle (Fig. 1C). Since the interaction with TPX2 is required for the stabilisation and complete activation of AurkA, we verified whether the increased amount of the complex yielded an up-regulation of its kinase activity. Indeed, while AurkA levels were increased both upon AurkA and AurkA/TPX2 overexpression, a strong increase of AurkA-Thr288 auto-phosphorylation is observed only in AurkA/TPX2 mitotic extracts (Fig. S1B); furthermore, this robust increase in auto-phosphorylation is not observed when AurkA is overexpressed with TPX2$^{\Delta 43}$ (Fig. S1B), defective for AurkA interaction [14,21]. By immunofluorescence (IF) we

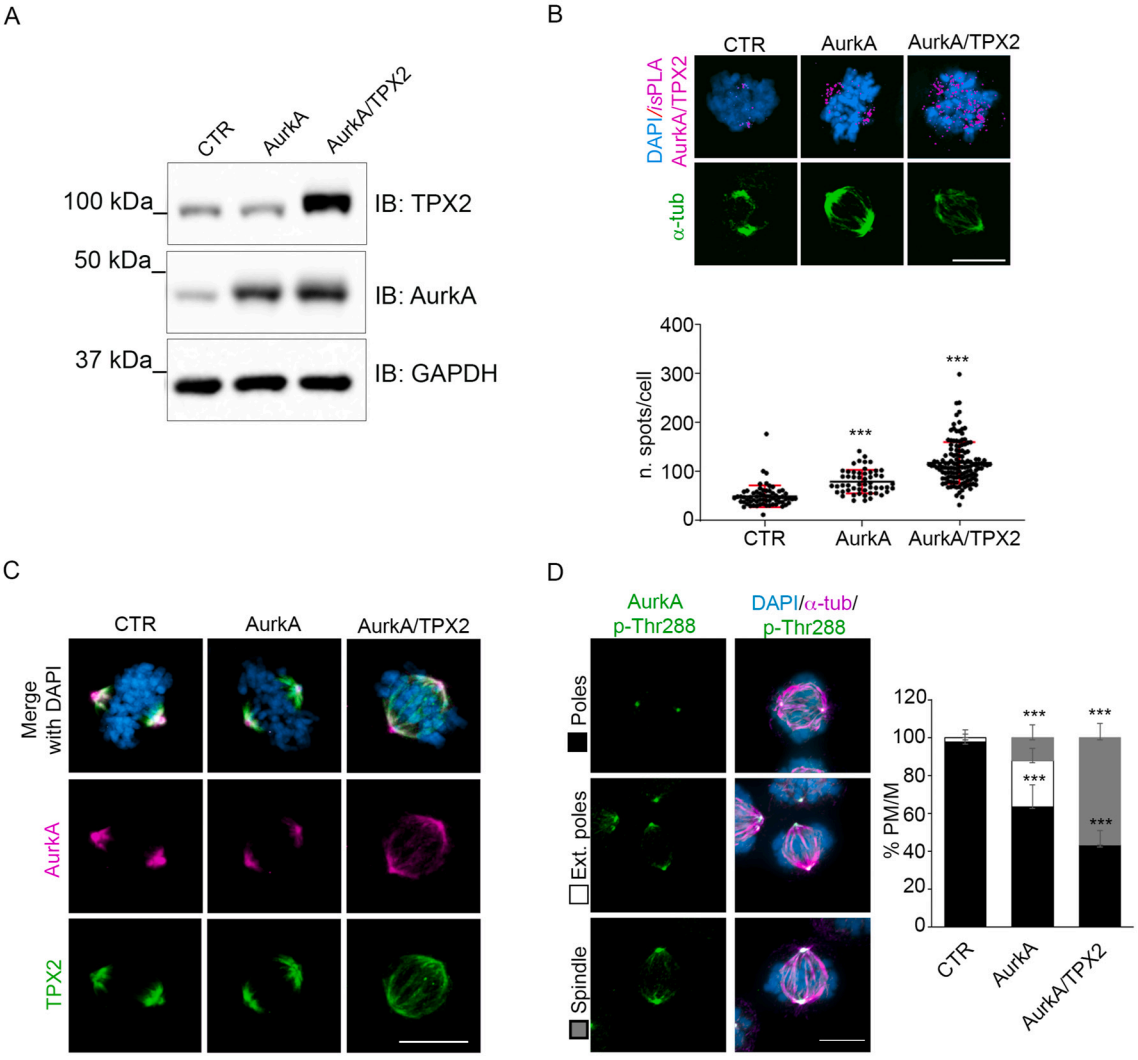

Fig. 1. AurkA/TPX2 co-overexpression determines mis-localisation and enhanced activity of AurkA in mitosis. (A) WB shows increased levels of AurkA and TPX2 in mitotic cells in the indicated cell lines (CTR are non-induced cultures). GAPDH was used as loading control. (B) Panels show representative examples of AurkA/TPX2 *is*PLA signals in mitotic cells from indicated cell lines, quantified (interaction spots per cell) in the dot plot below. (C) IF panels show representative images of the localisation of AurkA (magenta) and TPX2 (green) in mitotic cells in the indicated cell lines. (D) Histograms represent the different localisation patterns (exemplified in the IF panels) of p-Thr288 AurkA signal in prometa/metaphases (PM/Ms) in the indicated cell lines. Ext. poles: extended poles. At least 50 (B) and 150 (D) PM/Ms per condition, from 3 independent experiments, were analysed. Standard deviations are shown. ***$p < 0.0001$, Kruskal-Wallis (B) or χ^2 (Fisher's exact) (D) test. Scale bars: 10 μm. (For interpretation of the references to color in this figure legend, the reader is referred to the web version of this article.)

revealed that in the AurkA/TPX2 cells the phosphoThr288-AurkA (p-Thr288) signal was not restricted to centrosomes, as in CTR mitoses, but displayed a clear staining at MTs (Fig. 1D). These results indicate that co-overexpression of AurkA and TPX2 in nontransformed cells yields increased formation of the complex, resulting in mis-localisation and enhanced activity of AurkA with respect to overexpression of AurkA alone. Interestingly, a similar condition was described following inactivation of the PP6 phosphatase that targets AurkA within the AurkA/TPX2 complex, and was associated with chromosome mis-segregation, micronucleation and DNA damage [34,35], suggesting that unscheduled AurkA/TPX2 activity contributes to chromosomal instability.

In order to assess whether the differences observed in AurkA localisation and auto-phosphorylation state in AurkA- *vs* AurkA/TPX2 overexpressing mitoses resulted in distinct mitotic phenotypes, we analysed spindle structure and mitotic progression in the two cell lines. By staining MTs in IF experiments, we observed that following AurkA overexpression alone cells displayed a bipolar spindle structure comparable to control cells, while the majority of AurkA/TPX2 overexpressing mitoses had disorganised spindles (Fig. 2A), to a higher extent compared to what previously observed in the TPX2-only overexpressing cultures [26]. Concomitant analysis of the centrosomes, by visualising the pericentriolar material (PCM) component pericentrin, indicated that despite bipolar, mitotic spindles in about 23 % of AurkA overexpressing PM/Ms showed splayed poles containing fragmented PCM. Fragmentation of the PCM, also with foci scattered in the cell, was more frequently represented (about 70 % of PM/Ms) in the AurkA/TPX2 overexpressing cells (Fig. 2B). To investigate if multiple PCM spots reflected centriole abnormalities, we performed a pericentrin and centrin-1 costaining. In the large majority of PM/Ms. in both AurkA and AurkA/TPX2 overexpression conditions, 2 centriole pairs were present regardless of PCM fragmentation. Only upon AurkA/TPX2 co-overexpression a fraction of PM/Ms (15 %) displayed splitted centrioles in PCM fragmented spots (Fig. 2B), likely reflecting a strong loss of integrity of the centrosomes under this condition. To analyse whether this altered centrosome/spindle structure affected mitotic progression, we performed time-lapse video recording experiments. Consistent with the absence of strong spindle abnormalities, the cell line overexpressing AurkA alone underwent an apparently normal mitosis, with a small fraction of cells undergoing a slight delay in prometaphase (Fig. 2C-D). About 56 % of mitotic cells overexpressing AurkA/TPX2 instead underwent a strongly delayed prometaphase (average time from mitotic cell round up to chromosome segregation: 114′, compared to 17′ in control mitoses), similarly to what was observed in TPX2-only overexpressing mitoses [26]. Parallel analyses of fixed samples highlighted an accumulation of PM/M cells compared to control cultures (Fig. 2E), confirming a delayed progression through these mitotic substages. Nonetheless, only 8 % of the delayed mitoses resulted in mitotic failure while the large majority completed cell division (Fig. 2D), suggesting that these cells were eventually able to organise a pseudo-bipolar spindle, an ability often observed in cancer cells [5,36]. PM delay frequently results from defective MT-kinetochore attachments. Consistently, we found a significant increase in mis-aligned chromosomes in metaphase in AurkA/TPX2 overexpressing cells (Fig. 2F). In order to investigate the consequences of the PM/M defects observed upon AurkA/TPX2 co-overexpression on chromosome segregation fidelity, we analysed ana-telophases. About 15 % of AurkA/TPX2 overexpressing ana-telophases displayed lagging chromosomes, compared to about 6 % in AurkA overexpressing mitoses (Fig. 2G). Interestingly, in AurkA alone overexpressing cells, we observed chromosome bridges in about 15 % ana-telophases, a defect that was not significantly represented in cells overexpressing the whole AurkA/TPX2 complex (Fig. 2G). Neither chromosome bridges nor lagging chromosomes had been previously detected in TPX2-only overexpressing ana-telophases [26]. To rule out the possibility that the observed phenotypes were specific of hTERT RPE-1 cells, we generated a parallel set of AurkA or AurkA/TPX2 overexpressing cell lines in immortalised HFs (Fig. S2). Similar to what had been observed in RPE-1 cells, AurkA/TPX2 overexpressing mitoses, but not those overexpressing AurkA alone, accumulated in PM/M, displayed mis-aligned chromosomes in metaphase and lagging chromosomes in ana-telophase. Overexpression in HFs also confirmed the appearance of chromosome bridges in a fraction of anaphases overexpressing AurkA.

Overall results shown so far indicate that co-overexpressing TPX2 and AurkA produces significant differences in terms of AurkA localisation, activity and ensuing mitotic defects, compared to overexpression of the kinase alone.

3.2. Overexpression of the AurkA/TPX2 complex leads to kinase-dependent micronucleation

We then investigated the impact of the observed mitotic defects on the resulting progeny by performing, after 36 h of dox induction, metaphase spreads and interphase fluorescent *in situ* hybridization (FISH) analyses. Metaphase spread analysis revealed the occurrence of whole chromosome unbalances (Fig. 3A) in AurkA overexpressing cells, which were induced to a higher extent upon co-overexpression with TPX2. Consistent with our previous observations [26], cells overexpressing TPX2 alone did not differ from controls (Fig. S3A). For FISH analyses, we counted signals corresponding to chromosomes 7 and 8 in primary nuclei of asynchronously growing AurkA or AurkA/TPX2 overexpressing cells. We found a significant increase in cells aneuploid for either chromosome 7 or 8, or for both chromosomes, with a stronger defect in the AurkA/TPX2 co-overexpressing cell line (Fig. 3B). Parallel analyses of interphase nuclei visualised by DAPI confirmed a stronger induction of defects in the AurkA/TPX2 overexpressing cells, compared to the AurkA ones (Fig. 3C, left histograms): besides doughnut-shaped nuclei that we previously described as a result of TPX2 overexpression [26], a fraction of multinucleated cells appeared, likely originating from the delayed PM/Ms that exited mitosis without division (see Fig. 2D). Importantly, a significant fraction of cells displaying micronuclei, which were not detected in AurkA-only (Fig. 3C) or TPX2-only [26] overexpressing cultures, was also present (Fig. 3C), as also observed in AurkA/TPX2 overexpressing human fibroblasts (Fig. S2E). To directly link the appearance of these defects to the observed abnormal mitoses we repeated the analyses in a pure post-mitotic population, *i.e.*, the progeny of the first division after dox induction. Briefly, cells were synchronised at the G1/S transition by thymidine treatment and AurkA or AurkA/TPX2 overexpression was induced by dox administration at the time of thymidine wash-out. After 10 h (roughly corresponding to the mitotic peak) mitotic cells were collected by mechanical shake-off and re-plated, and samples were fixed after 4–5 h. Binucleation, a possible consequence of the shake-off procedure on telophase cells, was represented to a low extent under all conditions (Fig. S3B). Importantly, almost 15 % of resulting daughter cells in the AurkA/TPX2 overexpressing cultures displayed one or more micronuclei (Fig. 3C, right histograms). Data so far indicate the AurkA/TPX2 overexpressing condition as highly relevant for the generation of chromosomal unstable cells and particularly of micronuclei. Increased kinase activity of AurkA on MTs, due to the depletion of PP6 kinase, has been reported to generate micronuclei and numerical aneuploidy, fuelling genome instability in HeLa and melanoma cancer cells [34,35]. Together with our previous observation that in hTERT RPE-1 TPX2 overexpression *per se*, despite the strong effects on mitotic spindle assembly, did not affect chromosome segregation [26], this suggests that induction of genome instability in AurkA/TPX2 overexpressing cells might be due to TPX2-mediated unscheduled AurkA activation at the mitotic spindle. To address this issue, we selectively interfered with AurkA kinase activity by treating cultures with MLN8237 (Fig. 3D). We chose a low concentration of the inhibitor (1 nM), that did not impair physiological mitotic functions of AurkA in hTERT RPE-1, while restoring “near physiological” levels and localisation of p-Thr288-AurkA in mitotic AurkA/TPX2 overexpressing cells (Fig. S3C-F). After 24 h of dox induction and

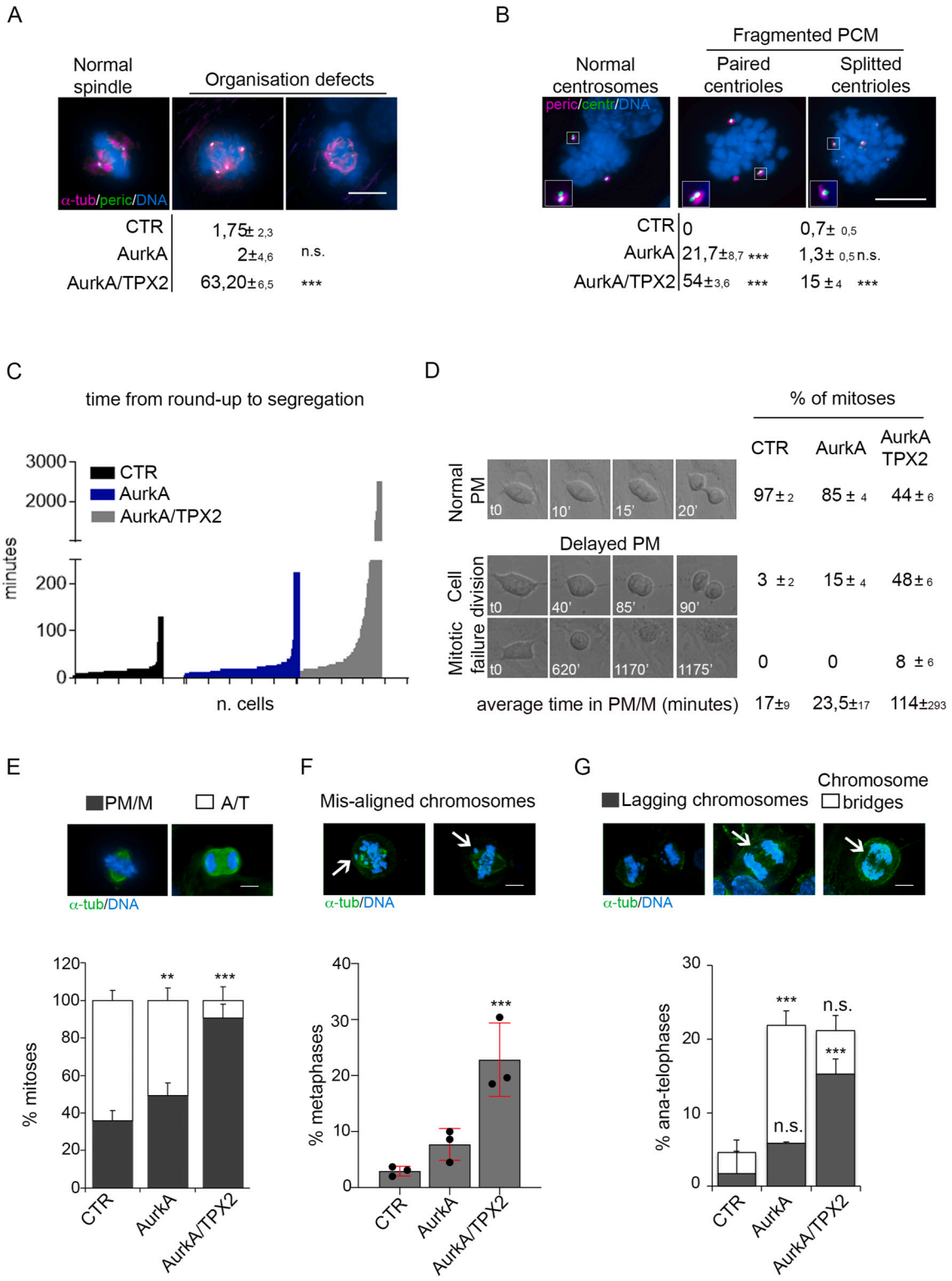

Fig. 2. Differential mitotic defects induced by increasing AurkA or AurkA/TPX2 levels. Mitotic spindle (A) or centrosomes (B) defects (representative examples in IF panels) were scored in PM/M in the indicated cell lines. The insets in B show enlargements of the centrin staining. (C) The graph represents the time (minutes) required from round up to the beginning of chromosome segregation, in the indicated cell lines, from time lapse data. Each line represents a single cell. Selected frames in (D) show a normal mitosis (top), or a delayed prometaphase, followed by either cell division (middle) or re-adhesion without chromosome segregation (bottom). Minutes from round-up (t0) are indicated. Phenotype percentages are shown in the table on the right. Cells spending more than "average control time + 2 standard deviations" in PM/M were considered as "delayed". (E) Histograms show the percentage of dividing cells in the mitotic sub-stages (PM/M and A/T, ana-telophases) in fixed samples, for the indicated cell lines. The percentage of mitotic chromosome defects scored in metaphase (F) and ana-telophase (G) are shown. Representative examples are shown for *E*-G in the corresponding IF panels. A total of about 300 cells were counted per condition, from 3 independent experiments in A-E; for F and G, at least 130 mitotic cells, from 3 independent experiments, were scored. Standard deviations are shown. n.s., not significant; $^{**}p < 0.001$; $^{***}p < 0.0001$, χ^2 (Fisher's exact) test. Scale bars: 10 μm.

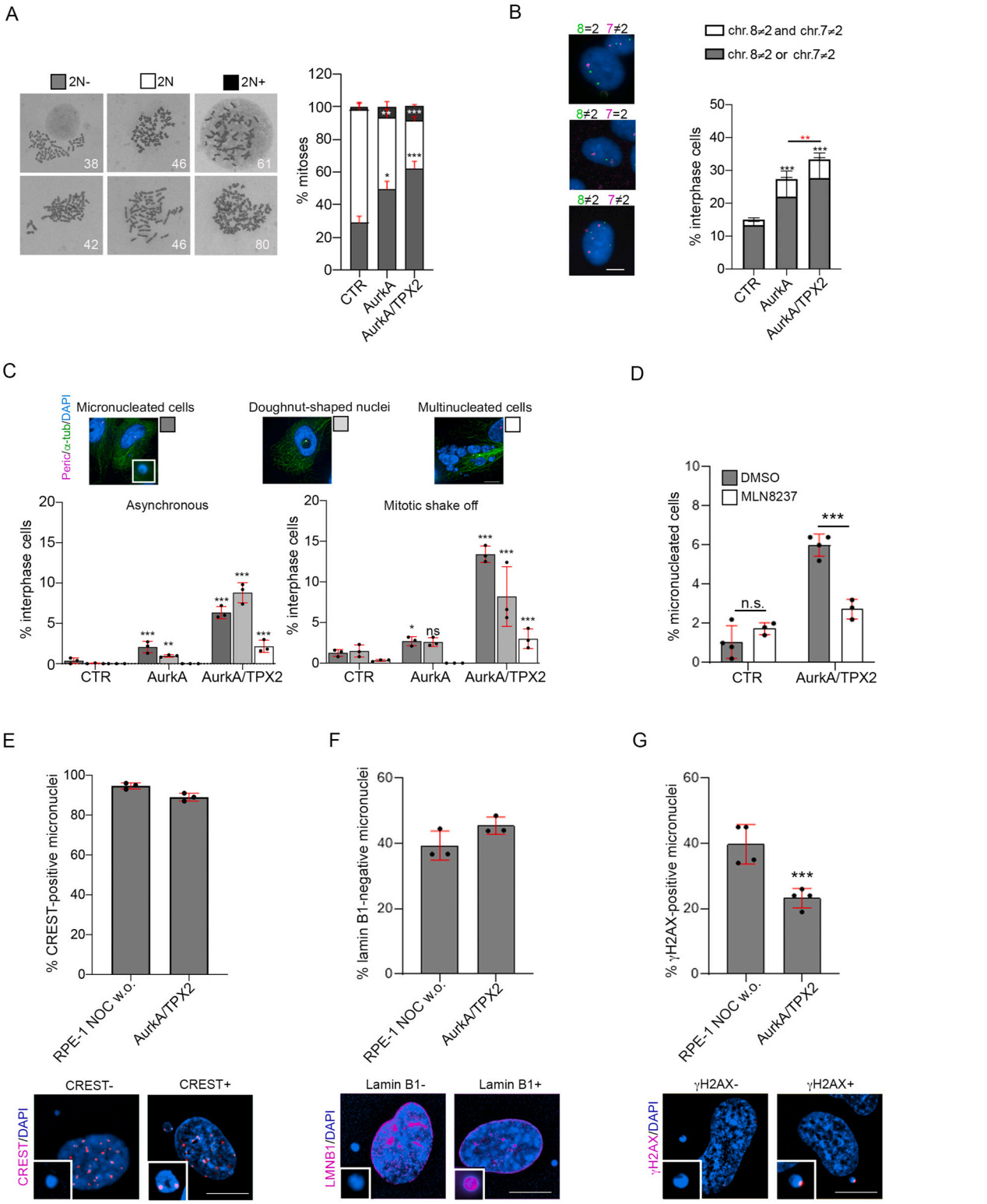

(caption on next page)

Fig. 3. The AurkA/TPX2 complex overexpression induces abnormal karyotypes and micronuclei in a kinase-dependent manner. (A) Histograms represent the percentage of cells with decreased (2N-) or increased (2N+) number of chromosomes compared to the euploid chromosome mitotic content (2N) in control (CTR), AurkA and AurkA/TPX2 overexpressing cells. Examples of the different classes are depicted in the left panels, and the number of chromosomes for each example is indicated. At least 62 metaphase spreads were analysed per condition, from at least 3 independent experiments. (B) Analysis by FISH in the indicated cell lines show the percentage of interphase cells aneuploid for either chromosome 7 (magenta) or 8 (green), or for both chromosomes. Primary nuclei were considered for the analysis (representative images of the 3 classes are shown in the panels on the left). At least 830 interphasic cells were scored from 3 independent experiments. Black asterisks refer to the difference from the control cells, red ones to the difference between AurkA and AurkA/TPX2 overexpressing cells. (C) Histograms show the percentage of nuclear defects scored in the indicated cell lines in asynchronous growing cultures (left histograms) and in post-mitotic cells (right histograms). IF images show the different scored defects; an enlargement of the micronucleus is shown in the inset. At least 1490 interphasic cells were analysed per condition, from at least 3 independent experiments. (D) The percentage of micronucleated cells in the indicated cell lines after DMSO or 1 nM MLN8237 treatment is represented. At least 1500 cells per condition were counted from 3 independent experiments. (E-G) Characterisation of AurkA/TPX2-generated micronuclei, compared to those induced in control cells upon nocodazole treatment (12 h)/washout (5 h), for the presence of kinetochores (E, CREST staining), nuclear envelope integrity (F, lamin B1 status) and DNA damage (G, γH2AX staining). IF images represent examples of the analysed classes. The insets show enlargements of the micronuclei. At least 760 micronuclei per condition, from 3 independent experiments, were analysed. Standard deviations are shown. n.s., not significant; $*p < 0.01$; $**p < 0.001$; $***p < 0.0001$. χ^2 (Fisher's exact) test. Scale bars: 10 μm. (For interpretation of the references to color in this figure legend, the reader is referred to the web version of this article.)

simultaneous MLN8237 treatment, we scored micronuclei, as a marker of mis-segregation events, in AurkA/TPX2 overexpressing cultures and found them significantly reduced compared to control (DMSO-treated) cultures (Fig. 3D). This result indicates that co-overexpression of TPX2 impairs chromosome segregation by increasing AurkA kinase activity, thus representing a source of micronucleation in nontransformed cells. Micronuclei are considered a CIN hallmark, prone to defective segregation in the subsequent mitosis [37,38], DNA damage [39] and nuclear envelope collapse [40], events that often result in extensive chromosomal rearrangements [41]. To further characterise micronuclei generated in the AurkA/TPX2 overexpressing cultures, we first analysed the presence of centromeric regions in these nuclear aberrations, by staining cells with the CREST (anti-centromere) antibody, to assess the presence of whole chromosomes trapped therein. As a control, we induced micronucleation in control cultures by nocodazole treatment/washout. In asynchronously growing cultures overexpressing the AurkA/TPX2 complex, the majority of micronuclei displayed one or more CREST dots (Fig. 3E), indicative of centromere-positive mis-segregating chromosomes. We then analysed the lamin B1 status, as a read-out of the nuclear lamina network integrity, and γH2AX apposition, as a marker of DNA damage, in the micronuclei. About 50 % of micronuclei in AurkA/TPX2 overexpressing cultures displayed a discontinuous or absent lamin B1 rim (Fig. 3F), indicative of a compromised nuclear envelope, suggesting that micronuclei will undergo catastrophe [40]· Differently, only 20 % micronuclei displayed γH2AX foci (Fig. 3G): this result, together with the above evidence of whole chromosome mis-segregation events, is in agreement with the current idea that the transition through S phase is a step required for the induction of replicative stress-mediated DNA damage in micronuclei [39,41]. These observations taken together support the idea that TPX2-mediated booster of AurkA kinase activity increases its genomic instability potential.

3.3. The p53/p21 response in AurkA/TPX2 overexpressing cells is affected in an AurkA-dependent manner

Data so far indicate that AurkA/TPX2 co-overexpression results in perturbation of chromosome segregation in hTERT-immortalised, genetically stable human nontransformed cells. However, aberrant cells generated by an altered mitosis are generally arrested in their proliferation in the subsequent G1 phase [42]. Interestingly AurkA is a well-known negative regulator of p53, a key surveillance factor to preserve genome integrity [43,44]. This evidence suggests the intriguing possibility that overexpression of AurkA and TPX2 on the one hand generates aberrant post-mitotic cells with micronuclei, prone to genome instability, while on the other hand affects the p53 response, enabling their proliferation. To explore this possibility, we first assessed whether overexpression of the AurkA/TPX2 complex generally affects the p53/p21-mediated response, by using camptothecin (CPT) to induce DNA damage and p53 stabilisation. WB, IF and RT-PCR analyses indicated an impaired response to CPT treatment, as assessed by (i) a slight decrease in p53 protein levels (more evident in the single cell analyses of IF images), with no fluctuations in p53 mRNA levels under basal or CPT treatment conditions in all analysed cell lines (Fig. 4A and Fig. S4A-C); (ii) an impaired accumulation of p21, compared to CPT-treated control cells, at both the protein and mRNA levels, (Fig. 4A and Fig. S4A-C), consistent with the role of AurkA in the inhibition of p53 transcriptional functions. These effects were observed also in cells overexpressing AurkA alone (Fig. 4A and Fig. S4A-C). Since AurkA phosphorylation of p53 has been reported to regulate both p53 stability and transcriptional function [43,44], we treated cultures with Nutlin-3, an inhibitor of the E3 ubiquitin ligase MDM2, the main negative regulator of p53. Indeed, although Nutlin-3 treated cells displayed a partial restoration of p53 levels when comparing control and AurkA or AurkA/TPX2 overexpressing conditions, p21 levels remained low, confirming an additional effect of the kinase overexpression on p53-mediated transcription (Fig. 4B and Fig. S4D).

We then analysed the stabilisation of p53, and the upregulation of p21 required for the cell cycle arrest, in micronucleated cells, hallmark of chromosomal instability scored in the AurkA/TPX2 overexpressing cells. Compared to the micronucleated cells in control cultures, those overexpressing the AurkA/TPX2 complex displayed a reduced signal intensity of both p53 and p21 (Fig. 4C). A similar effect on p21 levels was observed by WB analysis of overexpressing cultures analysed 24 h after nocodazole treatment/washout (Fig. 4D and Fig. S4E), when all cultures had exited mitosis, as indicated by the disappearance of cyclin B1 (Fig. S4F), which yielded comparable induction of micronuclei in control and AurkA/TPX2 overexpressing cultures (Fig. S4G). p53 stabilisation and ensuing p21 accumulation can occur in response to DNA damage in micronuclei or to preceding mitotic delay [42,45,46]. We therefore subjected control, AurkA and AurkA/TPX2 overexpressing hTERT RPE-1 cultures to monastrol treatment/washout, which yields similar levels of p53 compared to CPT treatment (Fig. S4H), to analyse their ability to respond to a similar extent of mitotic delay. Upon AurkA and AurkA/TPX2 overexpression IF analyses indicated an impaired response of the p53-p21 axis (Fig. S4I). To rule out the contribution of interphase cells within the population which have not undergone cell division, we repeated the analysis in a pure post-mitotic population by monastrol-arrest/shake-off and re-plate (protocol in Fig. S4L). Again, we observed a slight decrease of p53 levels accompanied by a significant reduction of p21 in both AurkA and AurkA/TPX2 overexpressing cells, compared to control cells (Fig. 4E and Fig. S4M). To analyse whether the observed impairment in p53-mediated response to altered mitosis is relevant for subsequent progression through the cell cycle, we analysed the ability of hTERT RPE-1 constitutively expressing AurkA and TPX2 by lentiviral vectors to proceed to S phase after nocodazole-mediated mitotic arrest/release. To this aim, we treated cultures with nocodazole for 12 h, then collected mitotic cells by shake-off, replated them in the presence of BrdU and analysed cultures every 24 h until 120 h [47].

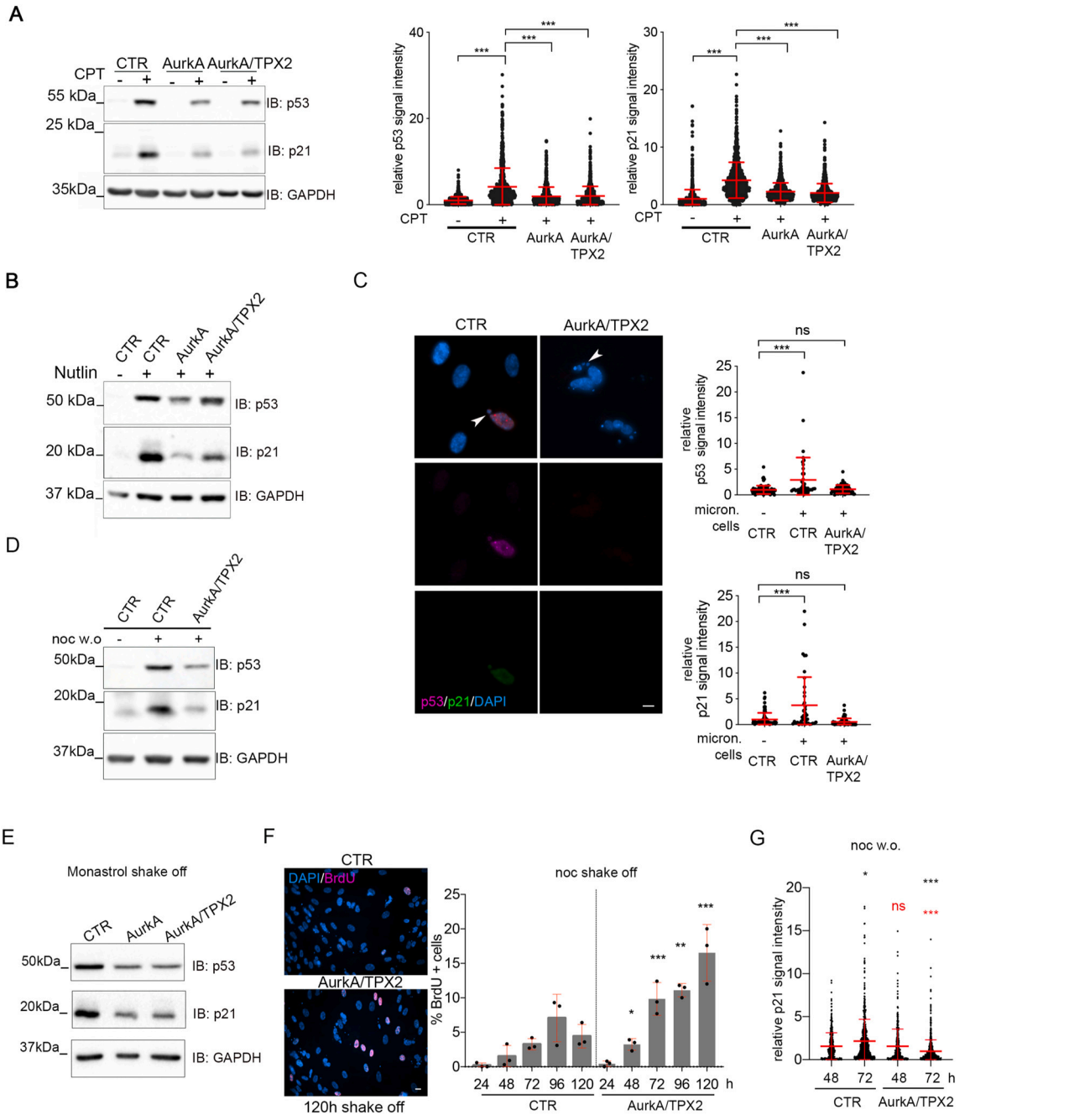

Fig. 4. The p53/p21 response to different stimuli is weakened in AurkA or AurkA/TPX2 overexpressing cells. (A) The WB on the left and the dot plots on the right (IF signal intensity) show p53 and p21 levels in the indicated cell lines after camptothecin (CPT) treatment or under basal conditions (−). At least 800 cells, from 3 independent experiments in each condition were analysed. (B) WB shows p53 and p21 levels in the indicated cell lines after Nutlin-3 treatment. (C) Dot plots on the right show the signal intensity of p53 and p21 inside primary nuclei of cells with (+) or without (−) micronuclei in the indicated cell lines. Examples are depicted on the left (arrowed micronuclei). At least 40 cells per condition from at least 3 independent experiments were analysed. (D) WB shows p53 and p21 levels in the indicated cell lines in asynchronously growing cultures (−) or after nocodazole washout (+). (E) WB showing p53 and p21 levels in the indicated cell lines after monastrol shake-off/replating. For the WB in A, B, D, E, GAPDH is the loading control. (F) Histograms represent the percentage of BrdU-positive cells at the indicated time points after nocodazole treatment, mitotic shake-off and replate in control and AurkA/TPX2 cell lines. On the left, IF representative images of BrdU signals in the cell cultures after 120 h from replate are shown. At least 560 interphasic per condition from at least 3 independent experiments were scored. Asterisks indicate the significance respect to the control culture at each time point. (G) The dot plot shows the analysis of p21 fluorescence signal intensity after nocodazole treatment/washout (time points are indicated) in control and AurkA/TPX2 overexpressing cells. At least 400 cells, per conditions from 3 independent experiments, were analysed. Red asterisks refer to the difference from the control cell line at each time, black ones to the difference between different time points within the same cell line. Standard deviations are shown. n.s., not significant; $*p < 0.01$; $**p < 0.001$; $***p < 0.0001$, Kruskal-Wallis ANOVA or χ^2 (Fisher's exact) (F) test. Scale bars: 10 μm. (For interpretation of the references to color in this figure legend, the reader is referred to the web version of this article.)

As expected, the percentage of BrdU positive cells remained around 5 % at all time points in control cultures. Instead, from 72 h of replating AurkA/TPX2 expressing cultures increasingly displayed BrdU incorporating cells, with about 15 % positive cells detected at 120 h (Fig. 4F). Consistently, p21 levels were significantly lower in parallel nocodazole arrested/released samples (Fig. 4G). These results support the hypothesis of weakened p53 control to mitotic aberrations upon AurkA/TPX2 overexpression, permitting the proliferation of cells that originated from altered cell division.

4. Discussion

Chromosome segregation is a crucial step in cell division, and not surprisingly altered expression of the master genes of the mitotic process represents a signature of chromosome instability in tumours [6], with the potential of driving cancer cells evolution and adaptation. In this study we focused on the AurkA and TPX2 mitotic regulators and on the effects of their co-overexpression, frequently observed in cancer [22], on the impairment of mitotic fidelity and its consequences. Indeed, despite AurkA being considered a proto-oncogene, investigation of its role in cell transformation reveals multifaceted and debated functions. Previous studies in cancer cell lines highlighted spindle and chromosome segregation defects upon AurkA overexpression, with some variability depending on the system [48,49], supporting the idea that additional deregulated genes in these cancer cell lines contribute to phenotype generation and that different genetic backgrounds may modulate the effects of AurkA overexpression on genome integrity. Similarly, despite TPX2 overexpression being associated with CIN and cancer [6,28,50] how it impacts chromosome segregation fidelity is not yet clarified. Recently, we reported that excess TPX2 in nontransformed cells does not induce lagging chromosomes or micronuclei, but rather affects nuclear envelope reassembly at mitotic exit [26]. Interestingly, the AurkA/TPX2 axis has been proposed as crucial for the survival of genomically unstable cancer cells [29] and a CIN4 including AurkA and TPX2, together with FOXM1 and TOP2A, associates with aneuploidy and tumour proliferation [28]. Supporting the importance of the AurkA/TPX2 complex in the generation of chromosomal instability in cancer, studies have shown that increased AurkA activity within the AurkA/TPX2 complex, due to PP6 depletion, induces lagging chromosomes and micronuclei [34], linked with the increased phosphorylation of NDC80 by AurkA [51]. Similar results were obtained in melanoma cells bearing PP6 inactivating mutations [35]. In the present study we analysed the consequences of overexpressing in nontransformed cells AurkA alone or AurkA/TPX2, both on AurkA activation and chromosome segregation fidelity. In our study, increased levels of AurkA lead to mild aneuploidy induction, consistent with results obtained in epithelial nontransformed MCF10A cells by transient transfection [52]. Instead, tetraploidy, reported for transient overexpression in murine embryonic fibroblasts [48], was not observed; this could be due to species-dependent outcomes, consistent with phenotypes observed in mouse models [53,54], or to different levels of overexpression yielded in transient *vs* stable and inducible expression. When TPX2 was co-overexpressed with AurkA we found that mis-aligned and lagging chromosomes increased compared to cells overexpressing AurkA alone, leading to stronger numerical aneuploidy and micronuclei generation, an event that rarely occurs in hTERT RPE-1 cells under unperturbed condition [55]. Interestingly, in our co-overexpression conditions we found an extended p-Thr288 AurkA signal at poles and spindle MTs, similarly to that observed as a PP6 depletion consequence in melanoma cancer cells [35]. This suggests that the AurkA/TPX2 co-overexpression overcomes the negative regulation of the complex by PP6 on spindle MTs. Consistent with the hypothesis that the mis-segregation events scored in our AurkA/TPX2 overexpressing cells are linked with the increased activation of AurkA, restoring its physiological activity with low doses of MLN8237 reduced micronuclei generation, as also occurred in PP6c depleted cells in previously published research [35]. On the contrary, mitotic delay was not rescued, supporting the idea of a strong contribution to this defect of TPX2 overexpression, as also indicated by results obtained with the TPX2 overexpressing cell line [26]. Based on observation carried out in PP6CKO cells we may speculate that defects observed in our system upon AurkA/TPX2 overexpression are somehow linked to aberrant phosphorylation of the NDC80 complex [51]. Another interesting possibility is that the abnormal distribution of active AurkA along spindle MTs disrupts the Aurora kinases gradient required for correct chromosome alignment and segregation [56,57], or that unscheduled AurkA activity in space and time impact on phosphorylation of AurkB substrates.

Interestingly, the presence of chromosome bridges in AurkA overexpressing cells suggests possible alterations occurring in S phase which may be linked to the newly discovered function of AurkA on replicative forks [58,59]. This defect may account for the aneuploidy scored in our AurkA overexpressing cell line. Given the complexity of the mechanisms through which DNA bridges can evolve in genome instability or rather be resolved [60–62], it will be interesting to investigate their origin, as well as their fate, in AurkA overexpressing conditions. On the other hand, the reduction of the defect when TPX2 has been co-overexpressed with the kinase, suggests potential protecting functions of TPX2 (or the AurkA/TPX2 complex) in DNA replication, as recently discovered [63,64]. This is a relevant observation in the light of the fact that AurkA and TPX2 are frequently co-overexpressed in tumours and that this is often due to chromosome 20q amplification [16], suggesting that the chromosome segregation defects and micronuclei generation observed in this study are a major source of genomic instability in those tumours.

Altered/failed mitosis, aneuploidy and micronuclei generation are strictly linked to DNA damage, replicative stress, multiple centrosomes and prolonged prometaphase, as a source and/or consequences of these defects [47,65–68]. Importantly, all these conditions can activate in several ways p53, the pivotal limit to genome alteration [45,47,67–70]. In addition, novel roles of p53 in control of proper execution of mitosis are emerging, supporting the idea of direct control on cell division [71]. Interestingly, while multinucleation induces a p53-independent cell cycle arrest [72], it has been recently shown that the depletion of p53 is sufficient to permit the proliferation of cells displaying micronuclei and/or altered nuclear shape [45,72]. Since AurkA is a well-known negative regulator of p53 [43], able to impair its stability and/or transcriptional activity, we explored the possibility that AurkA/TPX2 overexpression while inducing micronuclei also weakens the p53-mediated response to this defect. Indeed, we found reduced p53 levels in micronucleated cells overexpressing AurkA and TPX2. In addition, in our overexpressing cells, p53 stabilisation was reduced in response to several stimuli, such as DNA damage and mitotic delay, thus impairing p21 accumulation and enabling the progression of the cells to S phase after prolonged nocodazole arrest in prometaphase, that is normally limited. DNA damage, especially in micronuclei, has been linked with increased genetic alteration in nontransformed and cancer cells [41,62], suggesting that in our system the impaired cell cycle arrest due to AurkA activity can exacerbate the consequence of DNA breakage on genome integrity. In addition, this effect may be relevant in the response to chemotherapy in p53 proficient AurkA overexpressing tumours, supporting their survival to therapies despite the functional checkpoint system. The interplay between AurkA and p53-mediated pathways also deserve consideration and in-depth investigation in the light of the active research on the development of AurkA kinase inhibitors and their ongoing evaluation in clinical trials for cancer therapy [73]. Furthermore, these evidence

suggest that increased levels of AurkA can support cell transformation by limiting the p53 response in the presence of oncogenes that impairs genome integrity, as Myc family protein, well known positive regulators of AurkA expression [74,75]. These results are apparently in contrast with previous studies suggesting impaired proliferation of tetraploid p53 proficient cells [48] and reduced transforming ability [54] after human AurkA overexpression, conditions both rescued by p53 depletion. Both studies are in mouse-derived models, suggesting limited effects of human AurkA on murine p53. Interestingly, recent evidence supports the idea that murine and human p53 are differently regulated in mitosis [31]. A non-mutually exclusive possibility comes from the observation that both mentioned studies [48,54] describe a polyploidization step that we do not observe under our conditions in human cells; since different mechanisms regulate p53 in response to distinct mitotic and post-mitotic defects [71] this may indicate that AurkA overexpression impacts on specific p53 stabilisation pathways acting on upstream regulators. On note, the centrosome fragmentation phenotype observed in both our AurkA and AurkA/TPX2 overexpressing cell lines has also been observed in nontransformed human cells upon impairment of p53 mitotic centrosomal localisation, which is emerging as a sensor for the mitotic surveillance pathway [31]. This observation opens the possibility of more complex yet to be explored links between AurkA and p53 in mitosis.

Another puzzling observation is that, despite the differential activation level, in our system the impairment of p53 response occurs to a similar extent in AurkA and AurkA/TPX2 overexpressing cells. This would suggest that even a subtle increase in AurkA activity is *per se* sufficient to unbalance the p53-mediated surveillance pathway in a nontransformed human background. We cannot rule out that the observed effect is kinase-independent, although data in the literature would favour the hypothesis of phosphorylation-dependent mechanisms [43]. Finally, we cannot exclude the possibility that recently emerging links of TPX2 with the DNA damage response, involving direct interaction and modulation of key factors such as 53BP1, PARP1, H2AX contribute to the effects that we observe in the AurkA/TPX2 overexpressing cell line [63,64,76]. The involvement of AurkA in these newly identified functions is not clarified yet, leaving open the possibility that excess AurkA and TPX2 act through multiple, not mutually exclusive mechanisms to modulate the cellular response to genomic imbalances and DNA damage.

In conclusion, we found that AurkA overexpression alone in nontransformed cells yields a basal induction of aneuploidy that is increased in presence of TPX2 excess. Consistent with other studies [35,51], this result supports the idea of altered AurkA kinase activity as a driver of genome instability. It is also in line with the intriguing hypothesis, proposed previously by our group [22], that TPX2 is required -and sufficient- to deregulate AurkA activity, when co-overexpressed, and that this altered function is a main route for the kinase to impair chromosome segregation fidelity. On other hand, our results suggest that co-overexpression of AurkA may underlie chromosomal instability reported in TPX2-overexpressing tumours. These findings, together with our observation of an AurkA-dependent p53 impaired background, support the notion that the AurkA/TPX2 complex can drive chromosomal instability in situations where its expression is deregulated, *e.g.*, chromosome 20q amplification or Myc overexpression, and can represent a possible target to limit CIN in cancer cells.

CRediT authorship contribution statement

Francesco Davide Naso: Writing – review & editing, Writing – original draft, Visualization, Supervision, Resources, Investigation, Formal analysis, Conceptualization. **Federica Polverino:** Writing – review & editing, Writing – original draft, Visualization, Supervision, Resources, Investigation, Formal analysis, Conceptualization. **Danilo Cilluffo:** Visualization, Investigation. **Linda Latini:** Investigation. **Venturina Stagni:** Resources, Investigation. **Italia Anna Asteriti:** Visualization, Investigation. **Alessandro Rosa:** Resources. **Silvia Soddu:** Writing – review & editing, Writing – original draft, Resources, Conceptualization. **Giulia Guarguaglini:** Writing – review & editing, Writing – original draft, Supervision, Project administration, Funding acquisition, Conceptualization.

Declaration of competing interest

The authors declare that they have no known competing financial interests or personal relationships that could have appeared to influence the work reported in this paper.

Data availability

Data will be made available on request.

Acknowledgments

We thank Pietro Cirigliano for technical help with imaging experiments at the IBPM-Nikon Reference Center, Enrico Cundari, Cinzia Rinaldo, Francesca Degrassi and Catherine Lindon for useful scientific discussions, Anna Mastrangelo and Irene Mariani for experimental support. Research was supported by AIRC (IG-2021 ID: 25648 to G Guarguaglini and IG-2020 ID: 24403 to S Soddu); Regione Lazio (PROGETTI DI GRUPPI DI RICERCA 2020 project ID: A0375-2020-36597 to G Guarguaglini) and MUR (PRIN2022 project 2022N3JXLA to G Guarguaglini). The implementation of the microscopy infrastructure was supported by MUR (Ministry of University and Research) funds to the PON project “IMPARA, Imaging from molecules to the preclinics”. Work partially supported by CNR project FOE-2021 DBA.AD005.225.

Appendix A. Supplementary data

Supplementary data to this article can be found online at https://doi.org/10.1016/j.bbadis.2024.167116.

References

[1] S.F. Bakhoum, B. Ngo, A.M. Laughney, J.A. Cavallo, C.J. Murphy, P. Ly, et al., Chromosomal instability drives metastasis through a cytosolic DNA response, Nature 553 (2018) 467–472.
[2] W.H.M. Hoevenaar, A. Janssen, A.I. Quirindongo, H. Ma, S.J. Klaasen, A. Teixeira, et al., Degree and site of chromosomal instability define its oncogenic potential, Nat. Commun. 11 (2020) 1–11.
[3] A.E. Tijhuis, S.C. Johnson, S.E. McClelland, The emerging links between chromosomal instability (CIN), metastasis, inflammation and tumour immunity, Mol. Cytogenet. 12 (2019) 17.
[4] S.F. Bakhoum, W.T. Silkworth, I.K. Nardi, J.M. Nicholson, D.A. Compton, D. Cimini, The mitotic origin of chromosomal instability, Curr. Biol. 24 (2014) 148–149.
[5] W.T. Silkworth, D. Cimini, Transient defects of mitotic spindle geometry and chromosome segregation errors, Cell Div 7 (2012) 19.
[6] S.L. Carter, A.C. Eklund, I.S. Kohane, L.N. Harris, Z. Szallasi, A signature of chromosomal instability inferred from gene expression profiles predicts clinical outcome in multiple human cancers, Nat. Genet. 38 (2006) 1043–1048.
[7] I. Pérez de Castro, G. de Cárcer, M. Malumbres, A census of mitotic cancer genes: new insights into tumor cell biology and cancer therapy, Carcinogenesis 28 (2007) 899–912.
[8] A.W. Bird, A.A. Hyman, Building a spindle of the correct length in human cells requires the interaction between TPX2 and Aurora A, J. Cell Biol. 182 (2008) 289–300.
[9] V. Joukov, A. De Nicolo, Aurora-PLK1 cascades as key signaling modules in the regulation of mitosis, Sci. Signal. 11 (2018) eaar4195.
[10] O.J. Gruss, M. Wittmann, H. Yokoyama, R. Pepperkok, T. Kufer, H. Silljé, et al., Chromosome-induced microtubule assembly mediated by TPX2 is required for spindle formation in HeLa cells, Nat. Cell Biol. 4 (2002) 871–879.
[11] T.A. Kufer, H.H.W. Silljé, R. Körner, O.J. Gruss, P. Meraldi, E.A. Nigg, Human TPX2 is required for targeting Aurora-A kinase to the spindle, J. Cell Biol. 158 (2002) 617–623.
[12] M. De Luca, P. Lavia, G. Guarguaglini, A functional interplay between Aurora-A, Plk1 and TPX2 at spindle poles: Plk1 controls centrosomal localization of Aurora-A and TPX2 spindle association, Cell Cycle 5 (2006) 296–303.

[13] M. Giubettini, I.A. Asteriti, J. Scrofani, M. De Luca, C. Lindon, P. Lavia, et al., Control of Aurora-A stability through interaction with TPX2, J. Cell Sci. 124 (2011) 113–122.
[14] R. Bayliss, T. Sardon, I. Vernos, E. Conti, Structural basis of Aurora-A activation by TPX2 at the mitotic spindle, Mol. Cell 12 (2003) 851–862.
[15] N.M. Levinson, The multifaceted allosteric regulation of Aurora kinase A, Biochem. J. 475 (2018) 2025–2042.
[16] A.H. Sillars-Hardebol, B. Carvalho, M. Tijssen, J.A.M. Belien, M. de Wit, P.M. Delis-van Diemen, et al., TPX2 and AURKA promote 20q amplicon-driven colorectal adenoma to carcinoma progression, Gut 61 (2012) 1568–1575.
[17] W.F. Ooi, A. Re, V. Sidarovich, V. Canella, N. Arseni, V. Adami, G. Guarguaglini, et al., Segmental chromosome aberrations converge on overexpression of mitotic spindle regulatory genes in high-risk neuroblastoma, Genes Chromosom. Cancer 51 (2012) 545–556.
[18] I.P. de Castro, M. Malumbres, Mitotic stress and chromosomal instability in cancer: the case for TPX2, Genes Cancer 3 (2012) 721–730.
[19] S.M. Gomes-Filho, E.O. Dos Santos, E.R.M. Bertoldi, L.C. Scalabrini, V. Heidrich, B. Dazzani, et al., Aurora A kinase and its activator TPX2 are potential therapeutic targets in KRAS-induced pancreatic cancer, Cell. Oncol. (Dordr) 43 (2020) 445–460.
[20] S. Udhaya Kumar, A. Balasundaram, V. Anu Preethi, S. Chatterjee, G. V. Kameshwari Gollakota, et al., Integrative ontology and pathway-based approach identifies distinct molecular signatures in transcriptomes of esophageal squamous cell carcinoma, Adv. Protein Chem. Struct. Biol. 131 (2022) 177–206.
[21] I.A. Asteriti, F. Polverino, V. Stagni, V. Sterbini, C. Ascanelli, F.D. Naso, et al., AurkA nuclear localization is promoted by TPX2 and counteracted by protein degradation, Life Sci. Alliance 6 (2023) e202201726.
[22] I.A. Asteriti, W.M. Rensen, C. Lindon, P. Lavia, G. Guarguaglini, The Aurora-A/TPX2 complex: a novel oncogenic holoenzyme? Biochim. Biophys. Acta Rev. Cancer 1806 (2010) 230–239.
[23] M. Janeček, M. Rossmann, P. Sharma, A. Emery, D.J. Huggins, S.R. Stockwell, et al., Allosteric modulation of AURKA kinase activity by a small-molecule inhibitor of its protein-protein interaction with TPX2, Sci. Rep. 6 (2016) 1–12.
[24] I.A. Asteriti, F. Daidone, G. Colotti, S. Rinaldo, P. Lavia, G. Guarguaglini, et al., Identification of small molecule inhibitors of the Aurora-A/TPX2 complex, Oncotarget 8 (2017) 32117–32133.
[25] M. Orth, K. Unger, U. Schoetz, C. Belka, K. Lauber, Taxane-mediated radiosensitization derives from chromosomal missegregation on tripolar mitotic spindles orchestrated by AURKA and TPX2, Oncogene 37 (2018) 52–62.
[26] F.D. Naso, V. Sterbini, E. Crecca, I.A. Asteriti, A.D. Russo, M. Giubettini, et al., Excess TPX2 interferes with microtubule disassembly and nuclei reformation at mitotic exit, Cells 9 (2020) 374.
[27] J. Rohrberg, D. Van de Mark, M. Amouzgar, J.V. Lee, M. Taileb, A. Corella, et al., MYC dysregulates mitosis, revealing cancer vulnerabilities, Cell Rep. 30 (2020) 3368–3382.e7.
[28] A.M. Szász, Q. Li, A.C. Eklund, Z. Sztupinszki, A. Rowan, A.M. Tokés, et al., The CIN4 chromosomal instability qPCR classifier defines tumor aneuploidy and stratifies outcome in grade 2 breast cancer, PLoS One 8 (2013) e56707.
[29] S.E. van Gijn, E. Wierenga, N. van den Tempel, Y.P. Kok, A.M. Heijink, D.C. J. Spierings, et al., TPX2/Aurora kinase A signaling as a potential therapeutic target in genomically unstable cancer cells, Oncogene 38 (2019) 852–867.
[30] F. Polverino, F.D. Naso, I.A. Asteriti, V. Palmerini, D. Singh, D. Valente, et al., The Aurora-A/TPX2 axis directs spindle orientation in adherent human cells by regulating NuMA and microtubule stability, Curr. Biol. 31 (2021) 658–667.e5.
[31] C. Contadini, L. Monteonofrio, I. Virdia, A. Prodosmo, D. Valente, L. Chessa, et al., P53 mitotic centrosome localization preserves centrosome integrity and works as sensor for the mitotic surveillance pathway, Cell Death Dis. 10 (2019) 1–16.
[32] V. Stagni, A. Kaminari, Z. Sideratou, E. Sakellis, S.A. Vlahopoulos, D. Tsiourvas, Targeting breast cancer stem-like cells using chloroquine encapsulated by a triphenylphosphonium-functionalized hyperbranched polymer, Int. J. Pharm. 585 (2020) 119465.
[33] K.J. Livak, T.D. Schmittgen, Analysis of relative gene expression data using real-time quantitative PCR and the 2−ΔΔCT method, Methods 25 (2001) 402–408.
[34] K. Zeng, R.N. Bastos, F.A. Barr, U. Gruneberg, Protein phosphatase 6 regulates mitotic spindle formation by controlling the T-loop phosphorylation state of Aurora A bound to its activator TPX2, J. Cell Biol. 191 (2010) 1315–1332.
[35] D. Hammond, K. Zeng, A. Espert, R.N. Bastos, R.D. Baron, U. Gruneberg, et al., Melanoma-associated mutations in protein phosphatase 6 cause chromosome instability and DNA damage owing to dysregulated Aurora-A, J. Cell Sci. 126 (2013) 3429–3440.
[36] M. Kwon, S.A. Godinho, N.S. Chandhok, N.J. Ganem, A. Azioune, M. Thery, et al., Mechanisms to suppress multipolar divisions in cancer cells with extra centrosomes, Genes Dev. 22 (2008) 2189–2203.
[37] M. Soto, I. García-Santisteban, L. Krenning, R.H. Medema, J.A. Raaijmakers, Chromosomes trapped in micronuclei are liable to segregation errors, J. Cell Sci. 131 (2018) jcs214742.
[38] B. He, N. Gnawali, A.W. Hinman, A.J. Mattingly, A. Osimani, D. Cimini, Chromosomes mis-segregated into micronuclei contribute to chromosomal instability by missegregating at the next division, Oncotarget 10 (2019) 2660–2674.
[39] K. Crasta, N.J. Ganem, R. Dagher, A.B. Lantermann, E.V. Ivanova, Y. Pan, et al., DNA breaks and chromosome pulverization from errors in mitosis, Nature 482 (2012) 53–58.
[40] E.M. Hatch, A.H. Fischer, T.J. Deerinck, M.W. Hetzer, Catastrophic nuclear envelope collapse in cancer cell micronuclei, Cell 154 (2013) 47.
[41] C.Z. Zhang, A. Spektor, H. Cornils, J.M. Francis, E.K. Jackson, S. Liu, et al., Chromothripsis from dna damage in micronuclei, Nature 522 (2015) 179.
[42] J.D. Orth, A. Loewer, G. Lahav, T.J. Mitchison, Prolonged mitotic arrest triggers partial activation of apoptosis, resulting in DNA damage and p53 induction, Mol. Biol. Cell 23 (2012) 567–576.
[43] Kaori Sasai, Warapen Treekitkarnmongkol, H.K. Kazuharu Kai, S. Sen, Functional significance of Aurora kinases–p53 protein family interactions in cancer, Front. Oncol. 6 (2016) 247.
[44] H. Katayama, K. Sasai, H. Kawai, Z.M. Yuan, J. Bondaruk, F. Suzuki, et al., Phosphorylation by aurora kinase A induces Mdm2-mediated destabilization and inhibition of p53, Nat. Genet. 36 (2004) 55–62.
[45] M. Soto, J.A. Raaijmakers, B. Bakker, D.C.J. Spierings, P.M. Lansdorp, F. Foijer, R. H. Medema, p53 prohibits propagation of chromosome segregation errors that produce structural aneuploidies, Cell Rep. 19 (2017) 2423–2431.
[46] C.S. Fong, G. Mazo, T. Das, J. Goodman, M. Kim, B.P. O'Rourke, et al., 53BP1 and USP28 mediate p53-dependent cell cycle arrest in response to centrosome loss and prolonged mitosis, eLife 5 (2016) e16270.
[47] Y. Uetake, G. Sluder, Prolonged prometaphase blocks daughter cell proliferation despite normal completion of mitosis, Curr. Biol. 20 (2010) 1666–1671.
[48] P. Meraldi, R. Honda, E.A. Nigg, Aurora-A overexpression reveals tetraploidization as a major route to centrosome amplification in p53−/− cells, EMBO J. 21 (2002) 483–492.
[49] N. Ertych, A. Stolz, A. Stenzinger, W. Weichert, S. Kaulfuß, P. Burfeind, et al., Increased microtubule assembly rates influence chromosomal instability in colorectal cancer cells, Nat. Cell Biol. 16 (2014) 779–791.
[50] I.P. de Castro, M. Malumbres, Mitotic stress and chromosomal instability in cancer: the case for TPX2, Genes Cancer 3 (2012) 721–730.
[51] T. Sobajima, K.M. Kowalczyk, S. Skylakakis, D. Hayward, L.J. Fulcher, C. Neary, et al., PP6 regulation of Aurora A – TPX2 limits NDC80 phosphorylation and mitotic spindle size, J. Cell Biol. 222 (2023) e202205117.
[52] H. Zhou, J. Kuang, L. Zhong, W.L. Kuo, J.W. Gray, A. Sahin, et al., Tumour amplified kinase STK15/BTAK induces centrosome amplification, aneuploidy and transformation, Nat. Genet. 20 (1998) 189–193.
[53] D. Zhang, T. Hirota, T. Marumoto, M. Shimizu, N. Kunitoku, T. Sasayama, et al., Cre-loxP-controlled periodic Aurora-A overexpression induces mitotic abnormalities and hyperplasia in mammary glands of mouse models, Oncogene 23 (2004) 8720–8730.
[54] X. Wang, Y.X. Zhou, W. Qiao, Y. Tominaga, M. Ouchi, T. Ouchi, et al., Overexpression of aurora kinase A in mouse mammary epithelium induces genetic instability preceding mammary tumor formation, Oncogene 25 (2006) 7148–7158.
[55] A.M. Gomes, B. Orr, M. Novais-Cruz, F. De Sousa, J. Macário-Monteiro, C. Lemos, et al., Micro- nuclei from misaligned chromosomes that satisfy the spindle assembly checkpoint in cancer cells, Curr. Biol. 32 (2022) 4240–4254.e5.
[56] A. Ali, P.T. Stukenberg, Aurora kinases: generators of spatial control during mitosis, Front. Cell Dev. Biol. 11 (2023) 1139367.
[57] H. Hochegger, N. Hégarat, J.B. Pereira-Leal, Aurora at the pole and equator: overlapping functions of Aurora kinases in the mitotic spindle, Open Biol. 3 (2013) 120185.
[58] T. Tsunematsu, R. Arakaki, A. Yamada, N. Ishimaru, Y. Kudo, The non-canonical role of Aurora-A in DNA replication, Front. Oncol. 5 (2015) 153403.
[59] E.G. Almeida, X. Renaudin, A.R. Venkitaraman, A kinase-independent function for AURORA-A in replisome assembly during DNA replication initiation, Nucleic Acids Res. 48 (2020) 7844.
[60] J. Pampalona, E. Roscioli, W.T. Silkworth, B. Bowden, A. Genescà, L. Tusell, et al., Chromosome bridges maintain kinetochore-microtubule attachment throughout mitosis and rarely break during anaphase, PLoS One 11 (2016) e0147420.
[61] H. Jiang, Y.W. Chan, Chromatin bridges: stochastic breakage or regulated resolution? Trends Genet. 40 (2024) 69–82.
[62] N.T. Umbreit, C.Z. Zhang, L.D. Lynch, L.J. Blaine, A.M. Cheng, R. Tourdot, et al., Mechanisms generating cancer genome complexity from a single cell division error, Science 368 (2020) eaba0712.
[63] A.K. Byrum, D. Carvajal-Maldonado, M.C. Mudge, D. Valle-Garcia, M.C. Majid, R. Patel, et al., Mitotic regulators TPX2 and Aurora A protect DNA forks during replication stress by counteracting 53BP1 function, J. Cell Biol. 218 (2019) 422–432.
[64] T. Mosler, H.I. Baymaz, J.F. Gräf, I. Mikicic, G. Blattner, E. Bartlett, et al., PARP1 proximity proteomics reveals interaction partners at stressed replication forks, Nucleic Acids Res. 50 (2022) 11600–11618.
[65] V. Passerini, E. Ozeri-Galai, M.S. De Pagter, N. Donnelly, S. Schmalbrock, W. P. Kloosterman, et al., The presence of extra chromosomes leads to genomic instability, Nat. Commun. 7 (2016) 1–12.
[66] T. Wilhelm, M. Said, V. Naim, DNA replication stress and chromosomal instability: dangerous liaisons, Genes 11 (2020) 642.
[67] S. Santaguida, A. Richardson, D.R. Iyer, O. M'Saad, L. Zasadil, K.A. Knouse, et al., Chromosome mis-segregation generates cell-cycle-arrested cells with complex karyotypes that are eliminated by the immune system, Dev. Cell 41 (2017) 638–651.e5.
[68] N.J. Ganem, H. Cornils, S.Y. Chiu, K.P. O'Rourke, J. Arnaud, D. Yimlamai, et al., Cytokinesis failure triggers hippo tumor suppressor pathway activation, Cell 158 (2014) 833–848.
[69] N.D. Lakin, S.P. Jackson, Regulation of p53 in response to DNA damage, Oncogene 18 (1999) 7644–7655.
[70] L.L. Fava, F. Schuler, V. Sladky, M.D. Haschka, C. Soratroi, L. Eiterer, et al., The PIDDosome activates p53 in response to supernumerary centrosomes, Genes Dev. 31 (2017) 34–45.

[71] M.S. Levine, A.J. Holland, The impact of mitotic errors on cell proliferation and tumorigenesis, Genes Dev. 32 (2018) 620–638.
[72] M. Hart, S.D. Adams, V.M. Draviam, Multinucleation associated DNA damage blocks proliferation in p53-compromised cells, Commun. Biol. 4 (2021) 451.
[73] R. Du, C. Huang, K. Liu, X. Li, Z. Dong, Targeting AURKA in cancer: molecular mechanisms and opportunities for cancer therapy, Mol. Cancer 20 (2021) 15.
[74] F. Zheng, C. Yue, G. Li, B. He, W. Cheng, X. Wang, et al., Nuclear AURKA acquires kinase-independent transactivating function to enhance breast cancer stem cell phenotype, Nat. Commun. 7 (2016) 10180.
[75] I. Roeschert, E. Poon, A.G. Henssen, H. Dorado Garcia, M. Gatti, C. Giansanti, et al., Combined inhibition of Aurora-A and ATR kinase results in regression of MYCN-amplified neuroblastoma, Nat. Cancer 2 (2021) 312–326.
[76] G. Neumayer, A. Helfricht, S.Y. Shim, H.T. Le, C. Lundin, C. Belzil, et al., Targeting protein for xenopus kinesin-like protein 2 (TPX2) regulates γ-histone 2AX (γ-H2AX) levels upon ionizing radiation, J. Biol. Chem. 287 (2012) 42206–42222.